Machine Learning & Artificial Intelligence for Robotics - Homework 0

Particle Filtering for 2D Localisation

October 14th, 2019

Maurice Rahme

1 Part A

1.1 Designing the Motion Model

The subject being tracked by this particle filter is a mobile robot moving on a 2D plane. Access is not given to this robot's low-level controls (i.e differential drive actuation), so it is reasonable to assume a unicycle model whereby motion can be achieved by a combination of linear and angular velocity, thus mapping the robot as a 3 degree of freedom system represented by coordinates x, y, and θ. Hence, the nonlinear motion model used for this filter is the following for each iteration of time elapsed dt:

1. If w is zero:

$$x_t = x_{t-1} + v * cos(\theta_{t-1}) * dt + \epsilon_x \tag{1.1}$$

$$y_t+ = y_{t-1} + v * sin(\theta_{t-1}) * dt + \epsilon_y \tag{1.2}$$

2. If w is nonzero, we represent motion as a circular trajectory:

$$x_t+ = x_{t-1} + \frac{v}{w} * (-sin(\theta_{t-1}) + sin(\theta_{t-1} + w * dt)) + \epsilon_x \tag{1.3}$$

$$y_t+ = y_{t-1} + \frac{v}{w} * (cos(\theta_{t-1}) - cos(\theta_{t-1} + w * dt)) + \epsilon_y \tag{1.4}$$

$$\theta_t = \theta_{t-1} + w * dt + \epsilon_\theta \tag{1.5}$$

where v is linear velocity, ω is angular velocity, and ϵ is noise.

The model is nonlinear due to the sin and cos relationship between the robot coordinates and velocity [1].

1.2 Testing the Motion Model

In this basic test, the motion model updates the robot's state using the given commands. The resultant state is appended to a Path list which is used to plot the resultant trajectory in figure 1. This plot does not showcase the motion model's nonlinearity due to the decoupling of linear and angular velocity commands.

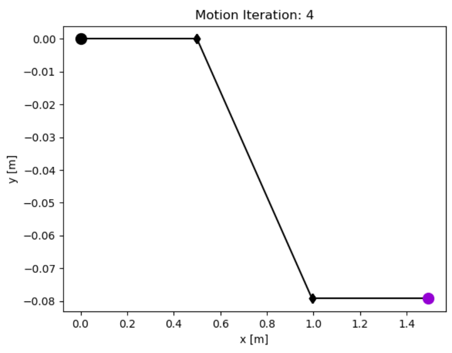

(a) Trajectory without Noise.

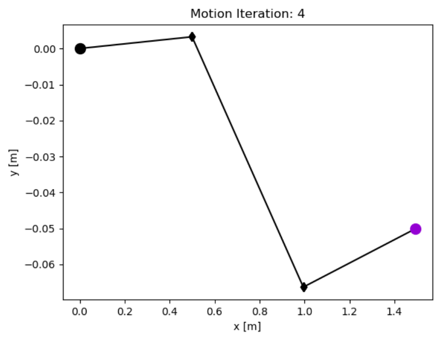

(b) Trajectory with Noise.

Figure 1: Testing the Motion Model.

1.3 Testing the Simulated Controller on the Robot Dataset

Here, the controls of the Odometry file in Data Set 1 were used to actuate the robot and plot its motion according to localisation by dead-reckoning. The data set does not provide values for dt, but it is easily extracted from the actuation time stamps, where $dt = t_{next} - t_{current}$. To better understand the localisation results, these were plotted against the values from the Ground Truth file provided by a camera in the robot's workspace in figure 2.

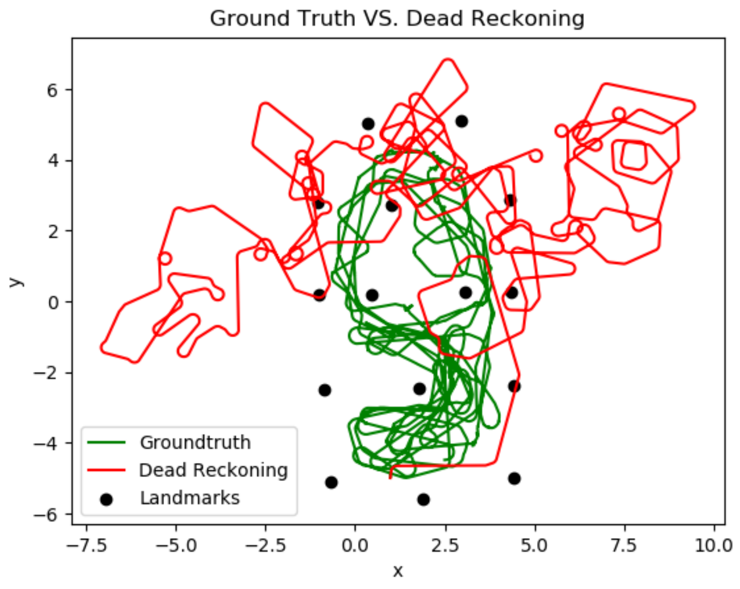

Figure 2: Dead Reckoning Pose Estimation VS Ground Truth Data, Full Set.

It is clear from this plot that the dead reckoning path diverges significantly from the ground truth path. To better identify this divergence, a plot limited at 2000 iterations can be printed, as shown in figure 3.

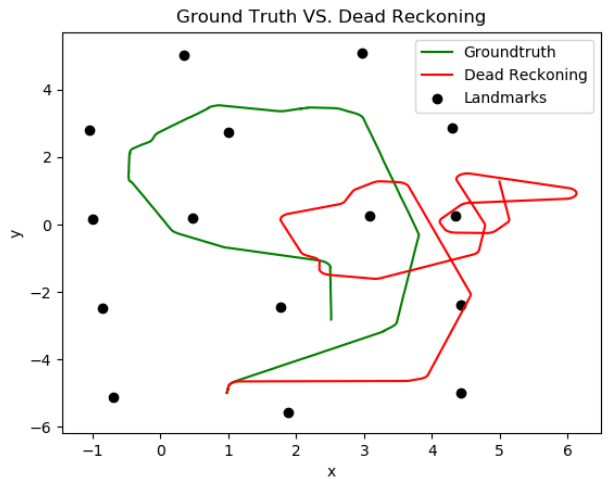

Figure 3: Dead Reckoning Pose Estimation VS Ground Truth Data, 2000 Iterations.

Examining the limited plot shows that the main source of discrepancy and error arises from the issuance of ω commands, as the dead reckoning data follows ground truth well during purely transnational motion, even recovering an initial offset due to a combination of rotational and transnational actuation done earlier.

1.4 Designing The Particle Filter

The Particle Filter is a nonparametric implementation of a Bayes filter, meaning that it computes the posterior $bel(x_t)$ of each state without needing to fit its data to a normal distribution. Instead, random state samples (particles) approximate this distibution. This filter is robust to occlusion, nonlinear dynamics, non-Gaussian noise, and most notably, it can represent multimodal posteriors, although this aspect of the filter is not needed here [2]. The filter algorithm is summarised in the following steps:

1. Generate Initial Particle Set according to the likelihood for a hypothesis to be included in set χ_t, which is proportional to posterior $bel(x_t)$: $x_t^{[m]} = p(x_t | z_{1:t}, u_{1:t})$, where z and u are measurements and controls respectively [2].

    (a) Knowing the robot's initial condition, generate M particles normally distributed around said position, setting the weight of each particle to $\frac{1}{M}$.

    (b) A tunable parameter here is the standard deviation in the coordinates of the generated particles.

2. Propagate each particle forward using the motion model described in section 1.1.

    (a) A tunable parameter here is control noise ϵ for w and v.

3. Perform weight update if measurement is recorded.

    (a) If a landmark measurement is recorded at any time interval between the current time stamp and the next (indicating that a measurement has occurred during the control step), calculate the expected range and bearing for each particle using equations 1.8 and 1.9. The smaller the difference between the recorded and predicted measurements for a given particle, the better that particle acts as a representation of true state. Hence, the weight assigned is the average of p^i_{range} and $p^i_{bearing}$ is described by equation 1.6 where r/b denotes the range or bearing estimated by the particle position, $\mu_{r/b}$ is the actual measure range or bearing, and σ^2 is the variance of the previous set, initialised to 1. If multiple measurements occur at a given time frame, average the weights assigned by each of them before normalising [2].

    $$p(r/b, \mu_{r/b}) = \frac{1}{\sqrt{2\pi\sigma^2}} \exp - \frac{(r/b - \mu_{r/b})^2}{2\sigma^2} \tag{1.6}$$

    (b) Normalise the weights of all particles by dividing each by the sum of all the weights so that they add up to 1. Note that in every iteration, the final weight is found by multiplying the weight of a given particle at the previous iteration with the its weight generated in this step [2].

4. Calculate w_{var}, the variance of the set's weights. A value tending to zero indicates that that all weights are converging to the same value, discouraging the use of a resampling step. Conversely, a high variance encourages resampling to redistribute the weights among weaker particles.

w_{var} is given by:

$$w_{var} = \frac{\sum(w_t^i - w_\mu))^2}{M - 1} \tag{1.7}$$

5. If w_{var} is above $4E - 10$, resample using Low-Variance resampling, which discards low-weight particles and replaces them with randomly generated ones.

    (a) Through a sequential stochastic process, the algorithm chooses a random number r, then - to build the new set - selects particles according to the weight-space division of $u = r + (m - 1) * M^{-1}$ as shown in figure 4 [2].

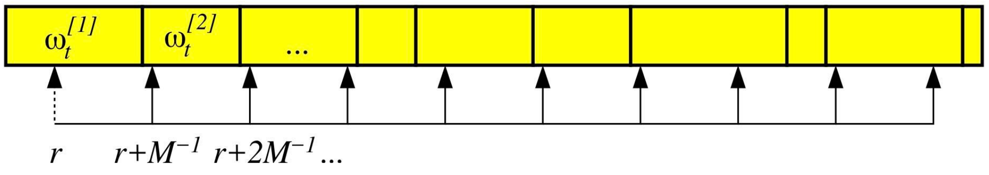

Figure 4: Low-Variance Resampling Weight-Space Division [2].

    (b) Within each division, the particle of index i selected is the one that corresponds to $c < u$, where $c = c + w_t^i$. Until this is true, i is incremented to evaluate the weight of the next particle in the division. Once the division is broken by $c < u$, the particle is added to the set and the next division is examined [2].

6. If w_{var} is below $0.2E - 10$ in the resampling step, generate $0.1 * M$ particles normally distributed around the prior to restore variance to the set. The values for w_{var} and the number of randomly generated particles was determined experimentally.

7. Extract the posterior from the sample set by computing a weighted average of x, y, and θ separately using the particle weights. The variance is extracted here for the next iteration using equation 1.7.

8. Repeat steps 2 through 7 for the entirety of the robot's motion.

A key design consideration is the number of particles, M. The particle filter is designed with a theoretical infinite sample set χ_t. The closer M tends to one, the less the measurement probability contributes to the weighing of particles due to an introduction of systematic bias to the posterior. This is evident in the extreme case of $M = 1$ where the single particle will always be taken as the posterior irrespective of its weight. However, increasing M increases computational power, so an intermediate value of 1000 was chosen to compromise between speed and performance. Increasing M also increases variance [2].

Another important factor is sample variance. This is especially true for Data Set 0, where the first measurement occurs only after 382 motion iterations, by which time the particles can easily converge to a single point due to the lack of measurements. This is the reason for which w_{var} is used to determine resampling, as well as the introduction of new random particles to the set as described in the algorithm [2].

1.5 Specifying the Measurement Model

The measurement model maps the range and bearing - as measured by the robot at various timestamps - to the cartersian position of the measured object (the landmark) relative to the robot, and vice versa. Notably, for the particle filter, given a landmark - whose cartesian position is known - the measurement model is used to compute the expected range and bearing of each particle in the active set. These expected readings are then compared to the actual reported sample, and are then used to assign a weight to each particle as described in section 1.4.

The model for expected range and bearing given known landmark and particle coordinates is given as follows [3]:

$$range = \sqrt{(x_t - xi - \epsilon_{xi})^2 + (y_t - yi - \epsilon_{yi})^2} \tag{1.8}$$

$$bearing = \arctan(\frac{y_i + \epsilon_{yi} - y_t}{x_i + \epsilon_{xi} - x_t}) \tag{1.9}$$

Where x_t, y_t denote the robot's cartesian coordinates, x_i, y_i denote the landmark's cartesian coordinates, ϵ_{x_i,y_i} is standard deviation of each landmark as reported by the Vicon camera, and ϵ_{x_t,y_t} is the robot's sensor noise, which was arbitrarily selected as 0.0001 as it is assumed to be worse than the Vicon camera, and no steady samples were provided to analytically compute noise.

1.6 Testing the Measurement Model

A simple test was conducted to assess the validity of the measurement model, whereby equations 1.8 and 1.9 were used to compute range and bearing respectively for known robot and landmark positions. These values were then fed into the complement of the measurement model, which computes the landmark position based on the robot's coordinates and the range and bearing computed by equations 1.8 and 1.9. The complement of the measurement model is described below:

$$x_i = x_t + range(\cos(bearing + heading)) \tag{1.10}$$

$$y_i = y_t + range(\sin(bearing + heading)) \tag{1.11}$$

Where $heading$ is simply the robot's orientation relative to the domain's x axis. Below are the results from running the test with and without measurement noise:

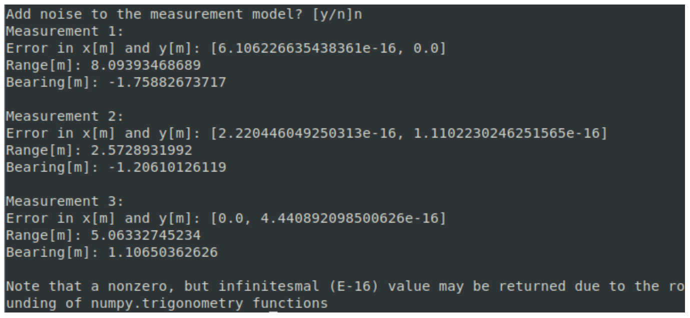

```
Add noise to the measurement model? [y/n]n
Measurement 1:
Error in x[m] and y[m]: [6.106226635438361e-16, 0.0]
Range[m]: 8.09393468689
Bearing[m]: -1.75882673717

Measurement 2:
Error in x[m] and y[m]: [2.220446049250313e-16, 1.1102230246251565e-16]
Range[m]: 2.5728931992
Bearing[m]: -1.20610126119

Measurement 3:
Error in x[m] and y[m]: [0.0, 4.440892098500626e-16]
Range[m]: 5.06332745234
Bearing[m]: 1.10650362626

Note that a nonzero, but infinitesmal (E-16) value may be returned due to the ro
unding of numpy.trigonometry functions
```

(a) Test without Noise.

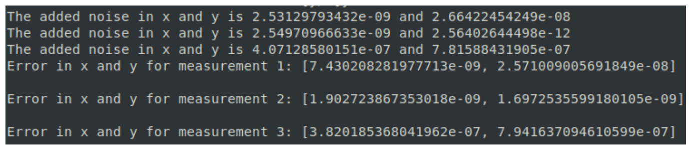

```
The added noise in x and y is 2.53129793432e-09 and 2.66422454249e-08
The added noise in x and y is 2.54970966633e-09 and 2.56402644498e-12
The added noise in x and y is 4.07128580151e-07 and 7.81588431905e-07
Error in x and y for measurement 1: [7.430208281977713e-09, 2.571009005691849e-08]

Error in x and y for measurement 2: [1.902723867353018e-09, 1.6972535599180105e-09]

Error in x and y for measurement 3: [3.820185368041962e-07, 7.941637094610599e-07]
```

(b) Test with Noise.

Figure 5: Testing the Measurement Model.

2 Part B

2.1 Assessing Filter Performance

2.1.1 Performance in the Basic Motion Test

If noise is added to the motion model for the commands in step 2, it deviates slightly from the expected trajectory. Conversely, as seen in figure 6, the particle filter traces a close trajectory even with the absence of measurements. However, this is not true for every instance, as it is sometimes less accurate than the dead reckoning path depending on the inherent randomness introduced by the particle set, which is not corrected by measurements in this case.

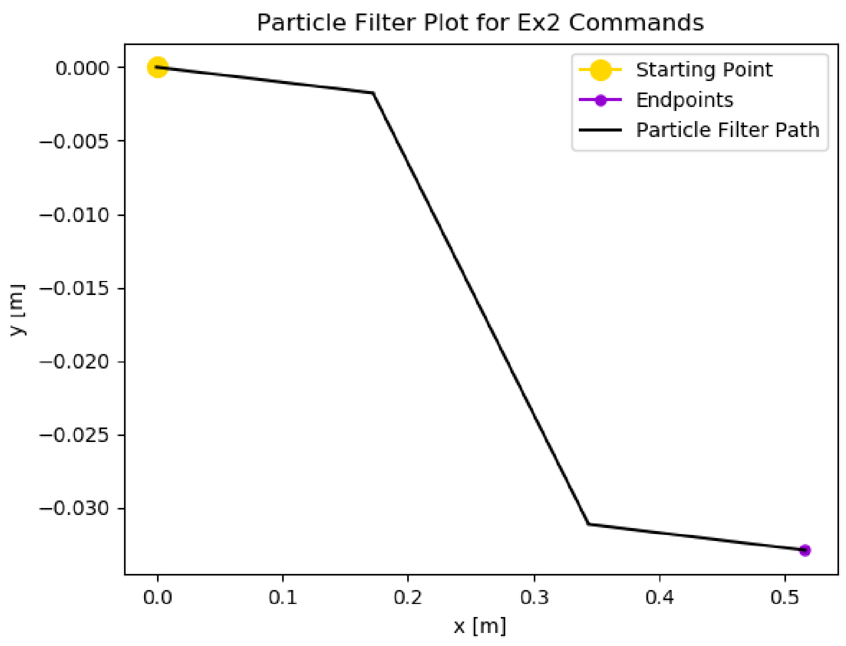

Figure 6: Particle Filter Trajectory for Exercise 2 Commands (With Noise).

2.1.2 Performance in the Odometry Data Test

Compared to dead reckoning, as shown in figure 7, the particle filter follows the ground truth path well. Note that the dead reckoning path behaved well in cases of near-total or total linear motion, but deviated significantly with the introduction of angular motion. Hence, in the initial particle distribution, the standard deviation for the x and y coordinates of the particles was kept low at 0.0002, but that of θ was kept comparatively higher at 1.5 so that particles would be able to explore a larger sample space of θ possibilities, as this was the main source of error. Although some tuning can be done to more narrowly follow the path, the chosen parameters were successful.

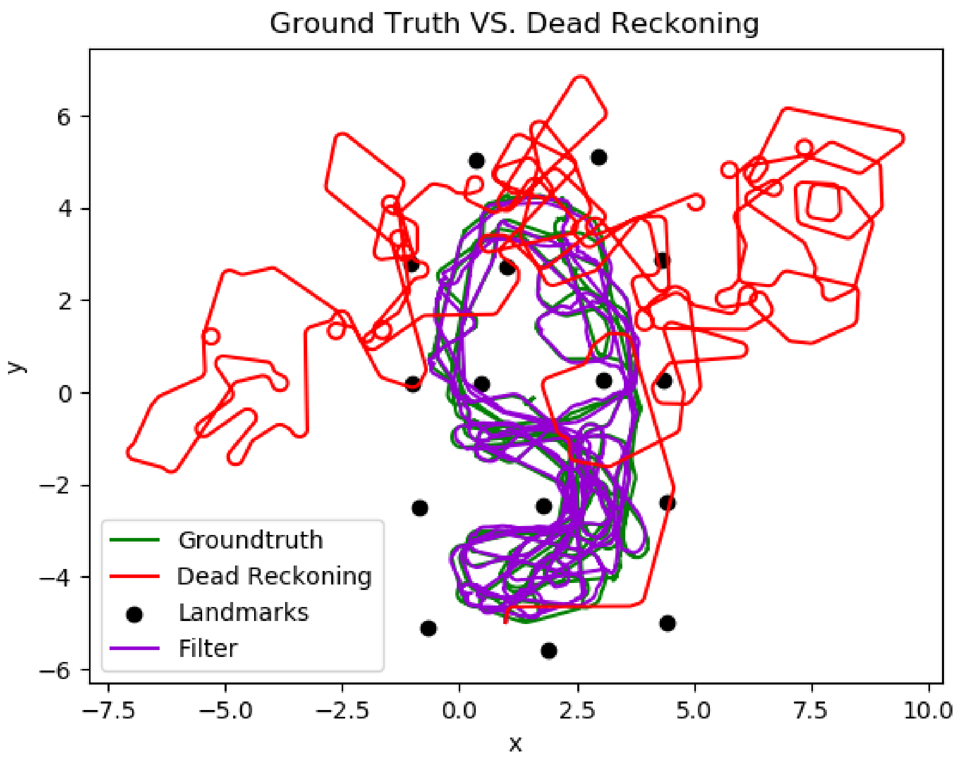

Figure 7: Particle Filter VS Ground Truth Path.

Noting that the weight update is performed using a measurement, clear attempts to correct at these time stamps can be identified by the jagged nature of the particle filter path in figure , post-correction. This means that an increase in measurement frequency could result in a smoother and more accurate path.

2.2 Uncertainty in the Algorithm

The filter produced here is effective, but could use some further tuning. There are many parameters to optimise, including motion model noise, sensor noise, the w_{var} threshold for resampling, the standard deviation of the initial normally distributed sample set, and the sample set size. With this variety of optimisation routes, it was difficult to identify a clear design procedure. However, certain elements showed more promise, notably the standard deviation of θ_t around the prior in both the initially generated set and the random sample replacements in the resampling stage. A higher comparative value of 1.5 to 2, depending on other parameters, showed better performance as it geared the particle filter to evaluate particles mainly using their bearing measurement, hence correcting the rotational motion deviation mentioned in section 1.3. Below are plots for θ of 1.5 and 2 respectively.

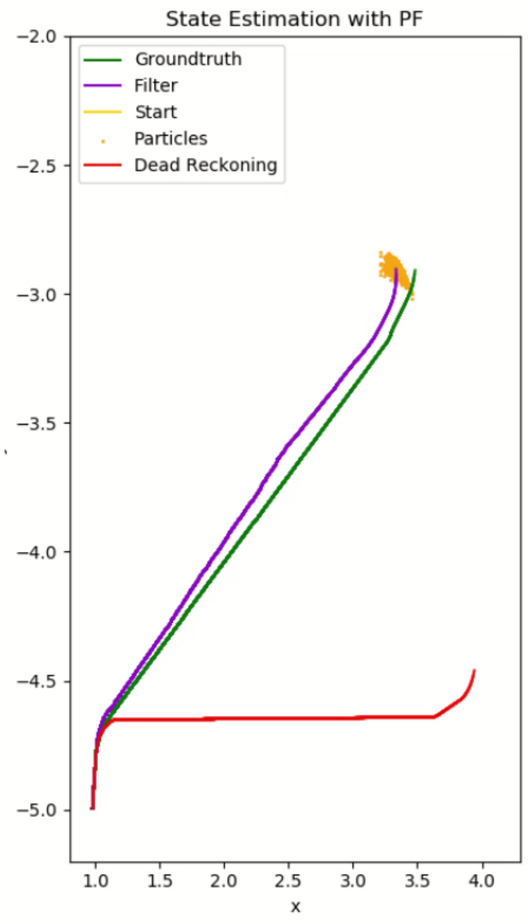

(a) Path before measurement

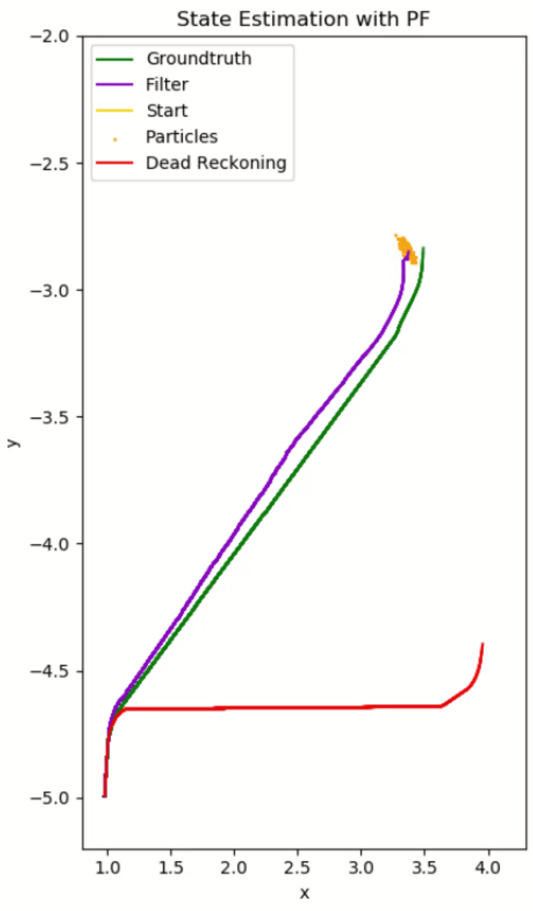

(b) Path after measurement

Figure 8: Pre and post measurement path.

Notably, here, it is evident that the prior belief loses confidence prior to the measurement as shown by a larger particle spread. This is promptly corrected once the measurement is taken, abruptly correcting the path and narrowing the particles.

Another important variable was found to be w_{var}, as this determined the resampling frequency. The chosen minimum of $4E-10$ for resampling and maximum of $2E-10$ for introducing radom particles into the resampling were chosen experimentally, but could be further optimised by examining the outcome of resampling and particle introduction frequency over various portions of the control set. In tandem, the number of random particles to be generated in the special resampling step is another tunable parameter with a significant effect on performance.

Ultimately, the filter performed well and as expected. It does follow the path well, but could use some further tuning for smaller error. Notably, the filter was crucial during rotational velocity commands, but less so for purely linear motion. Arguably, it could be said that the filter hinders upon dead reckoning estiation for linear motion as it struggles the estimate a straight-line path when that is clearly what the ground truth is doing. This qualitative observation could be implemented in the algorithm such that the filter estimate is only considered during nonlinear

Notably, this trajectory is much smoother than those in figures 8 and 9. However, it is evidently a worse performer, highlighting the importance of the measurement update and the destabilising effect caused by its absence in the beginning of the control sequence. The later measurements are implemented, the longer the filter will take to recover. This is especially true if measurements are scarce.

Finally, note that the motion model used in section 1.1 is a unicycle model, and may not represent the detailed motion of the robot. This may also have an effect on performance, although it is recognised that the particle filter is robust against this issue. The frequency of measurements also plays an important role in the estimate, but those in the provided dataset were sufficient for producing a good path.

3 Citations

[1] "Robot Motion." Probabilistic Robotics, by Sebastian Thrun et al., MIT Press, 2010.

[2] "The Particle Filter." Probabilistic Robotics, by Sebastian Thrun et al., MIT Press, 2010.

[3] Russel, Stuart Norvig Peter. Artificial Intelligence: a Modern Approach. PEARSON, 2018.